Engineered Science
DOI: https://dx.doi.org/10.30919/es8d878

Artificial Neural Network Levenberg–Marquardt Based Algorithm for Compressive Strength Estimation of Concrete Mixed with Magnetic Salty Water

Mohammad Khorshidi Paji,[1] Behrouz Gordan,[2] Chiara Bedon,[3,*] Iman Faridmehr,[4] Kiyanets Valerievich[4] and Hyeon-Jong Hwang[5]

Abstract

Water quality and content significantly influence the mechanical properties of concrete. In light of the global water shortage, the utilization of seawater for concrete production has garnered considerable interest within the industry. Furthermore, sufficient compressive strength must be ensured for such an alternative. Magnetized seawater can be effectively employed for plain concrete production, thereby representing a sustainable construction material. In this investigation of Caspian Seawater, the magnetic parameters demonstrate a substantial impact on the concrete mixture's compressive strength. To accomplish this, the internal angles of hydrogen and oxygen atoms are initially altered during the magnetic treatment of saline water. In total, 364 concrete specimens were prepared for testing, with the critical water-to-cement ratio ranging from 0.45 to 0.55. Simultaneously, the magnetic field intensity (MFI) and water circulation time varied between 0.2-1.2 Tesla and 5-65 minutes, respectively. An artificial neural network combined with the Levenberg–Marquardt algorithm (ANN-LM) was employed to develop a novel hybrid model for evaluating the compressive strength samples. The innovative ANN-LM hybrid model was subsequently utilized in a sensitivity analysis to determine the fundamental parameters' influence on the compressive strength of concrete specimens.

Keywords: Magnetic water treatment; Compressive strength; Artificial neural network; Salty water.
Received: 04 February 2023; Revised: 01 May 2023; Accepted: 01 May 2023.
Article type: Research article.

1. Introduction

Concrete is a suitable material for construction buildings, and it is mainly applied because of some important factors such as high compressive strength, flowability, durability, and versatility. Water is essential to cement hydration processing, allowing it to act as the main binder for concrete. Considering the global water shortage, water management is necessary for the concrete industry and sustainable construction. The earth's water is fresh; just 3% and 2.5% of the Earth's freshwater is unavailable to extract from different places such as glaciers, polar ice caps, atmosphere, and soil as highly polluted under the earth's surface with a high level of cost to extract.

Magnetic water treatment is a technique of supposedly reducing the influences of hard water by passing water through a magnetic field as a non-chemical alternative to water softening. Previous studies demonstrated that magnetic water would increase some fresh and hardened concrete's properties, such as strength, workability, bleeding characteristics, and resistance to freezing and thawing.[1-3] Su and Wu[4] experimentally investigated the impact of magnetic field-treated water on the compressive strength of concrete mixture using fly ash. It was shown that the compressive strength prepared with tap water is generally lower than that mixed with magnetic treated one (with magnetic field intensity (MFI) of 0.2-1.35 Tesla). Additionally, the greatest growth in compressive strength was obtained, especially in the early stage, using magnetic water treated at 0.8 and 1.2 Tesla. Consequently, switching freshwater to magnetic water for concrete manufacturing represents a sustainable and efficient approach.

In recent years, a growing number of studies have been

[1] *Department of Civil Engineering, Chalous Branch, Islamic Azad University, Chalous, 4661934816, Iran.*
[2] *Department of Civil Engineering, Hamedan Branch, Islamic Azad University, Hamedan, 6518115743, Iran.*
[3] *Department of Engineering and Architecture, University of Trieste, Trieste, 34100, Italy.*
[4] *Department of Building Construction and Structural Theory, South Ural State University, Chelyabinsk, 454080, Russia.*
[5] *School of Architecture, Konkuk University, Seoul, 05029, Korea.*
**Email:* chiara.bedon@dia.units.it (C. Bedon)

done investigating the impact of magnetic water treatment on the mechanical properties of concrete. Ghorbani *et al*.[5] reported that the use of magnetized significantly improved the mechanical and durability behavior of concrete block pavers. Dharmaraj *et al*.[6] investigated the influences of magnetized water on mechanical and durability properties. They concluded that magnetic water for preparing samples and curing improved the compressive strength by 14.86% more than ordinary concrete. They also indicated that the consumption of chemical admixtures considerably decreased in magnetized water-imbibed concrete. Jouzdani and Reisi[7] investigated the impacts of water flow rate into an electromagnetic field (Q) and MFI on the mechanical properties of self-compacting concrete. They conclude that the compressive, bending, and tensile strengths were increased by up to 34.1%, 52.4%, and 74.2%, respectively, using magnetized water with MFI= 1.2 Tesla and Q= 9 Liter/min. They also confirmed that superplasticizer consumption decreased by 34.1% using that magnetized water properties. Magnetic water was also studied on early-age shrinkage cracking by Wei *et al*..[8] They confirmed that the total cracking area of the unit area and the strain rate factor for concrete were decreased, indicating the early-age shrinkage cracking resistance of concrete prepared by magnetized water is enhanced than those samples prepared with tap water. Furthermore, the effects of magnetized water on self-compacting concrete were investigated by Esfahani *et al*..[9] when keeping the dosage of superplasticizer constant and decreasing the water over cement ratio. They indicated that superplasticizer dosage could decrease by 30% when magnetized water is applied to self-compacting concrete.

The use of seawater for concrete mix is possibly a sustainable idea. Meanwhile, global warming and freshwater shortage suggest that this method will become conceivable. However, the existence of high concentrations of chloride impact by seawater would cause corrosion in steel reinforcement. Such a drawback can be overcome by using magnetized water for concrete mix or non-corrosive reinforcement (*i.e.*, carbon fiber reinforced polymer (CFRP) bars). The magnetic treatment affects the polarity of ions, which increases the permeability of chloride into the cellular membranes, which works to break down the salts and increases the readiness of the nutrients by breaking the salt crystals.[10] There is no systematic study in the open literature investigating for magnetized seawater impacts on the compressive strength of concrete.

In the present study, using Caspian Seawater, 364 specimens were prepared to investigate the effect of magnetic treatment parameters (*i.e.*, MFI and water circulation time) on compressive strength. Subsequently, an artificial neural network (ANN) coupled with Levenberg–Marquardt algorithm (ANN-LM) was used to develop a hybrid model to estimate the compressive strength of concrete prepared with magnetized Caspian Seawater. The ANN-LM was also employed to perform the sensitivity analysis and assess the influence of magnetic water treatment parameters on compressive strength.

2. Literature Review

2.1 Application of Magnetic Seawater for Concrete and Mortar

Nan Su *et al*. investigated the compressive strength and workability of mortar and concrete, which were mixed with magnetic water and contained granulated blast-furnace slag (GBFS).[11] They considered test variables, including the magnetic strength of water, the content of GBFS in place of cement, and the water-to-binder ratio (W/B). Results show that the compressive strength of mortar samples mixed with magnetic water of 0.8–1.35 T increased 9–19% more than those mixed with tap water. Alaa M. Rash and MohamedEzzat investigated the possibility of employing magnetic water, Zamzam water, and seawater as mixing water for alkali-activated slag pastes.[12] The results of workability, pH value, compressive strength, and microstructure of different specimens mixed with each type of water were compared with those mixed with tap water. They confirmed that magnetic water has the height improvement, followed by Zamzam water and seawater, respectively, whilst tap water came in the last place. Ramalingam Malathy *et al*. investigate the efficient utilization of magnetic water in M40 grade concrete and study the enhancement of its properties on hardened concrete and the structural behavior of prestressed concrete (PSC) beams.[13] They concluded that using magnetic water on pre-tensioned concrete beams improves flexural strength by 25%. Malathy Ramalingam investigated the influence of magnetic water on concrete properties with different magnetic field exposure times.[14] They concluded that there were 25.6% and 24.1% increments in workability and compressive strength, respectively, for the magnetic water at 60 min exposure periods compared to normal water concrete.

The present study aims to investigate the effects of magnetic treatment parameters on the compressive strength of concrete mixed with Caspian Seawater. Previous studies have shown that the use of magnetic water can improve the mechanical and durability properties of concrete. However, to the best of our knowledge, no systematic study has been conducted on the effects of magnetized seawater for plain concrete mix. Additionally, the study introduces a novel approach by employing the ANN-LM algorithm supported by Graphical User Interface (GUI) to estimate the compressive strength of concrete mixed with magnetic salty water. This hybrid model approach provides a more accurate and reliable prediction of compressive strength compared to traditional statistical models. Therefore, the current study contributes to the existing literature by providing new insights into the effects of magnetic treatment parameters on the compressive strength of concrete mixed with Caspian Seawater and by introducing a novel approach to predict the compressive strength of concrete using the ANN-LM algorithm.

2.2 Background of intelligent model in construction building materials

An Artificial Neural Network (ANN) is a developed mathematical model based on an organization of biological neural network cells of a living organism and the assumption of functioning. Currently, ANN models have been applied in order to solve diverse and difficult problems (*i.e.*, pattern recognition, speech recognition, and complex forecasts). At present, using ANN in countless fields of human activity is prevalent. Since ANN is the most commonly used artificial intelligence (AI) technique in different industries and sectors, including civil and architectural engineering, construction building materials, *etc*., a growing body of literature reviewing ANN applications have been published in recent decades. ANN models are generally applicable to an extensive dataset consisting of several input parameters and one or two output parameters, which is commonly included training (TR), validation (VAL), and testing subsets (TS). The training set is applied for model training and validated data provide an unbiased assessment of the model fit on training data and avoid overfitting by stopping the training procedure when the error rises. The model is finally used for the testing data to evaluate its prediction performance.

ANN are algorithms that can be employed to make non-linear numerical modeling and deliver a new alternative to logistic regression, the most frequently used technique for developing estimating models for dichotomous outcomes in engineering problems. ANN offers various advantages, demanding less formal statistical training, implicitly detecting complex non-linear relations between dependent and independent variables, detecting all possible interactions between predictor variables, and the availability of multiple training algorithms.[15] A precise estimate of the mechanical features of concrete and mortar has been a main concern since international design standards regularly require these properties. Developing novel concrete mixes and applications in this area has motivated scientists to develop ANN models to predict mechanical properties. Khosravani *et al*.[16] used an artificial intelligence (AI) system to estimate the dynamic properties of ultra-high-performance concrete (UHPC) constructed based on various mixtures. This ANN model was also deployed to predict elastic modulus, compressive strength, and tensile strength, all based on the high level of loading rate. Fan *et al*.[17] proposed a method for detailed design and characteristics estimate of UHPC compressive strength by using the modified Andreasen and Andersen (MAA) model and Genetic Algorithm based on Artificial Neural Network (GA-ANN) method. Van Dao *et al*.[18] developed two artificial intelligence methods, namely adaptive neuro-fuzzy inference (ANFIS) and ANN, to estimate the compressive strength of geopolymer concrete (GPC), where coarse and fine waste steel slag was applied for aggregates. Feng *et al*.[19] studied the application of artificial intelligence to assess the fresh properties of self-consolidating concrete. They concluded that the ANN technique was an excellent base to be combined with other optimization algorithms and an alternative for experimental techniques.

Previous studies confirmed that using ANN models to predict and produce concrete with expected strength at construction sites was a promising technique. These studies demonstrated the neural network-based technique's ability to predict compressive strength based on concrete mixture proportions. This process can contribute to preserving concrete quality based on optimal concrete mixtures. As the database containing mixed proportions and identified and tested strengths is accumulated over time, the ANN trained by this database will become more operative; also, the estimated result will become more reliable.

2.3 MLR model

Multiple linear regression (MLR) is a method largely employed in statistical analysis. Its objective is to calculate the expected result based on some variables, plotting the correlation between these multiple independent variables and single dependent variables. This model is based on a mathematical assumption as a linear relationship exists between independent and dependent variables. To perform a MLR analysis, it is necessary to put a few fundamental values in governing equation, that is:

$$y = b_0 + b_1x_1 + b_2x_2 + \cdots + b_px_p \quad (1)$$

$$\acute{y} = b_0 + b_1x_1 + b_2x_2 + \cdots + b_px_p \quad (2)$$

$$\varepsilon = y - \acute{y} \quad (3)$$

where y is observed data; $\acute{y}$ is predicted data; b_0 is y-intercept or value of y through all parameters set to 0; b_1x_1 is regression coefficient of the first independent variable; b_px_p is regression coefficient of the last independent variable; and ε is model error or level of variant. MLR is developed based on ordinary least squares technique (OLS), and the model is designed to minimize the sum of squares of differences among observed and predicted values. Fig. 1 shows the MLR flowchart.

The MLR is developed model based on some hypothesis (*i.e.*, errors are generally distributed with zero mean and constant variance). Providing that these assumptions are satisfied, the regression estimators are at optimum level because they are impartial, effective, and consistent. “Impartial” means that the estimator's expected value is equal to the parameter's actual value. “Effective” indicates that the estimator has a more minor variance than any other estimator. "Consistent" means that the variance and bias of the estimator tend to zero as the sample size tends to infinity.

2.4 ANN with Levenberg–Marquardt Algorithm (ANN-LM)

The Levenberg–Marquardt (LM) algorithm is used to determine non-linear least squares equations in engineering problematics.[20] This curve fitting technique combines two other methods, such as gradient descent and Gauss-Newton. Both methods included iterative algorithms, which means that they use several calculations (following estimates for *x*-values)

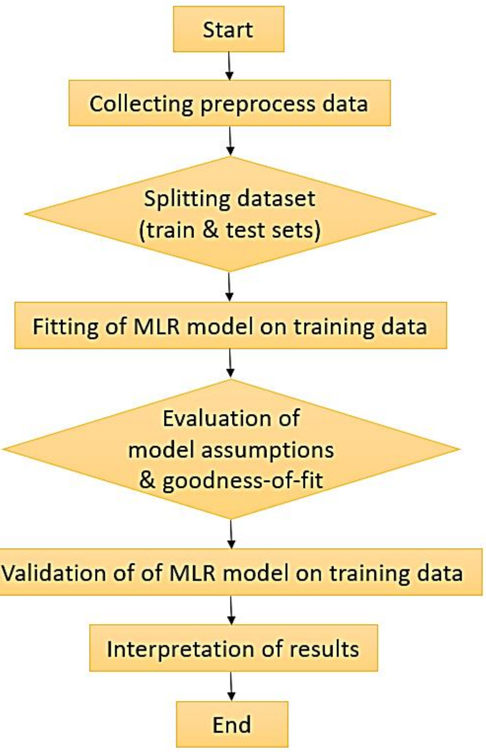

Fig. 1 Flowchart of MLR calculation approach.

to find the result. The descent of the gradient changes in each iteration; the solution updates by selecting values that make the function value minor. More exactly, the sum of the squared errors is decreased by moving in the direction of the steepest descent. The LM algorithm, which combines the gradient descent and Gauss-Newton methods, selects between these two methods for each iteration and updates the resolution.[21] Gradient descent is a first-order iterative optimization algorithm used to minimize a function by iteratively moving in the direction of the steepest decrease of the function. On the other hand, the Gauss-Newton method is an optimization algorithm used to solve non-linear least squares problems by linearizing the non-linear model function at the current parameter values and solving the resulting linear least squares problem. The iterative update process is determined by the value of an algorithmic parameter, λ, a non-negative damping factor that smooths the curve. The update follows the gradient descent path when λ is large, and the Gauss-Newton path when λ is small (*i.e.*, near to the optimum value).[22] As the Gauss-Newton method is more accurate and faster than the gradient descent method when close to the least error, the algorithm will shift towards the Gauss-Newton method as early as possible. The advantages of the LM algorithm can be listed as follows:

i. The LM algorithm provides a more accurate solution than the Gauss-Newton approach, as it offers two potential choices for the algorithm's path at each iteration;[23]
ii. The convergence rate is faster than either the Gauss-Newton or gradient descent methods alone. Convergence refers to the process by which an iterative algorithm approaches the optimal solution as the number of iterations increases;
iii. The LM algorithm can handle models with multiple factors that are not precisely identified;
iv. The algorithm can also find the best solution even when the initial guess has lower accuracy than the actual value.

The LM algorithm updates the ANN weights as in equation 4:[24]

$$\Delta w = [\mu I + \sum_{P=1}^{P} J^p(w)^T J^p(w)]^{-1} \nabla E(w) \tag{4}$$

where $J^p(w)$ is the Jacobian matrix of the error vector $e^p(w)$ calculated in w; and I is the identity matrix.

The error vector $e^p(w)$ is the error of the network for pattern p (*i.e.*, $e^p(w) = t^p - O^p(w)$). The parameter μ is climbed or declined at each step. If the error is decreased, μ is divided by a ratio β, and it is multiplied by β in other cases. It is noted that further information about LM algorithm can be found in the literature.[25]

3. Experimental Test and Method

3.1 Material

Cement type II manufactured by Shahroud, Iran, was used in this study. The adopted chemical and physical features for cement are listed in Table 1.

Table 1. Chemical and physical properties of shahroud cement (type 2) of Iran.

Chemical composition & phases (%)										
C_4AF	C_3S	C_2S	C_3A	LOI	SO_3	MgO	CaO	Fe_2O_3	Al_2O_3	SiO_2
11.9	54.6	19.5	6.3	2.18	1.73	1.33	63.58	3.92	4.87	21.18

Physical & mechanical test				
Blaine (cm^2/gr)	Retained on sieves (45μ)%	Setting time (min)		Compressive strength (MPa)
		Initial setting time	Final setting time	
3300	10	125	180	40.4

More precisely, for aggregate, the Zarrin-Gol mine of Aliabad-Katul city (which is located in northern Iran) was taken into account. The fine aggregate size was set between 0.7 and 2 mm, and the coarse aggregate was measured between 15 and 22 mm. Furthermore, the value of elastic modulus for fine aggregate was calculated in 80 GPa, which positively impacted the mechanical properties of concrete. Table 2 summarizes the characteristics of aggregates in use for the present investigation on magnetized concrete.

Table 2. Fine and coarse aggregate specifications.

Material	Specific gravity (t/m^3)	Water content (%)	Maximum diameter (mm)
Gravel	2.69	1.45	22
Sand	2.45	2.54	2

Seawater salinity is expressed as a ratio of salt (in grams) to a liter of water. In each liter of seawater, there are around 35 grams of dissolved salts. The Persian Gulf's salinity range ranges from 38 to 40 grams per liter. This index ranges in the coastal and middle coast of the Caspian Sea, including 14 and 11 grams per liter, respectively, and about 7 grams in the northern area. Besides, the low quantity of electrical conductivity (EC) for the northern area of the Caspian Sea is attributed to the two huge rivers, Dan and Volga, flowing from the Russian Federation and rivers flowing from four neighboring countries. The salinity index of Caspian Sea at the Iran border was around 14 grams per liter, which was used for concrete mixing after magnetic treatment in this study. Table 3 compares the chemical compositions of Ocean water against Caspian Seawater.[26]

Table 3. Chemical composition comparison of ocean water with Caspian seawater.[26]

Salt type	Percentage in the Caspian Sea	Percentage in the Ocean
NaCl	62.2	78.3
$MgSO_4$	23.6	6.40
$MgCl_2$, $MgBr_2$	4.54	9.44
$CaCO_3$	1.24	0.21
KCl	1.21	1.69
$CaSO_4$	6.92	3.93

3.2 Magnetic Water Production Treatment

A bespoke magnetizing water assembly fabricated for the present study was used to magnetize Caspian seawater, see Fig. 2. The assembly comprises a power supply that changes alternating current to direct current, so by generating a magnetic field produced by the current crossing through both ferrous cores wrapped around the coil, the water passes among the two nuclei and turns into magnetic. The magnitude of the magnetic field was adjusted using Tesla gauge, and the assembly had the selection of converting alternating current into direct current, adjusting voltage and amperage. The distance between both ferrous nuclei that were experimentally adjusted controlled the MFI in the range of 0.2 to 1.2 Tesla (0.2 Tesla interval). The magnetic water spins from the first tank to the secondary tank, ranging from 5 to 65 minutes (5 minutes' interval).

3.3 Testing Procedure and Establishing Dataset

Apart from magnetic water treatment parameters, the ratio for water over cement was also varied to prepare the mix designs. The cement content was fixed at either 300 or 400 kg/m^3, whereas the ratio was set at either 0.45 or 0.55. The slump of the sample made with freshwater was considered to regulate the water consumption in the samples made with magnetized water. Once the cube samples were cast in the mold and spent the setting time, they were demolded and cured in the freshwater pool for 28 days. After the curing period, the compressive strength of the samples was determined using a universal testing machine (UTM) under a controlled loading rate of 0.5 MPa/s, in accordance with the relevant standard. Fig. 3 shows the phases fulfilled to prepare samples for the compressive strength test. These phases include weighing the materials, concrete mixing, curing period, and subsequently compressive strength test.

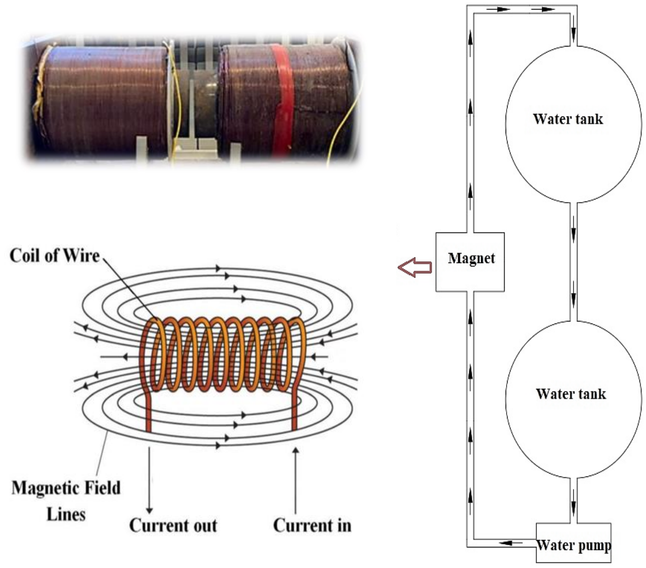

Fig. 2 Magnetic water production treatment.

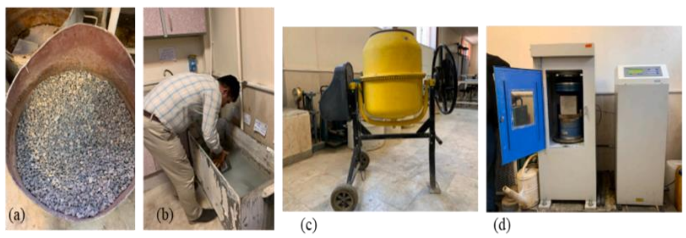

Fig. 3 Test setup (a) aggregate, (b) concrete mixture, (c) curing phase, (d) compressive strength test.

To develop a dataset for the informational models, static compression test was conducted on 364 concrete cubes after 7 and 28 days of curing. Table 4 summarizes the statistical information of tested samples.

Table 4. Statistical information of the tested samples.

Parameter	Category	Unit	Range	St. Deviation	Median
Cement content	Input	kg/m^3	300-400	50.06	350
Magnetic field	Input	Tesla	0-1.2	0.4	0.6
Water circulation time	Input	Minute	0-65	18.7	35
Water-to-cement ratio	Input	-	0.45-0.55	0.05	0.5
Compressive strength	Output	MPa	26.9-50.1	54.4	37.45

3.4 Application of ANN-LM model

3.4.1 Dataset

The dataset and its features are described in Section 3.3 above. In order to prepare a database, a total number of 364 compression tests were conducted on the samples, and their compressive strength values were recorded. In these tests, two cement contents have been used, such as 300 and 400 kg/m^3.

In addition, in these tests, magnetic field intensities of 0, 0.2, 0.4, 0.6, 0.8, 1, and 1.2 and water rotation times of 5, 10, 15, 20, 25, 30, 35, 40, 45, 50, 55, 60 and 65 min and water to cement ratios of 0.45 and 0.55 were applied. Therefore, in this study, cement content, magnetic field intensity, water rotation time, and water-to-cement ratio were selected to be used as model inputs to predict the compressive strength of concrete (*i.e.*, focused on 28 days).

The independent input variables in this dataset include the cement content, magnetic field intensity, water circulation time, and ratio of water over cement which produce a 4×1 matrix, while the dependent output factors contain the compressive strength of concrete, which develops a 1×1 matrix. The properties of input/output variables are given in Table 4.

Figure 4 shows this research's correlation matrix developed for input/output variables. In order to avoid any divergence in the results, the variables were first normalized in the range of 1 to -1 by using the following equation, where X_n is the normalized variable value, X_{max} and X_{min} is its maximum and smallest value, X is the non-transformed (original) value of the variable:

$$X_n = \frac{2(X - X_{\min})}{X_{max} - X_{mix}} - 1 \tag{5}$$

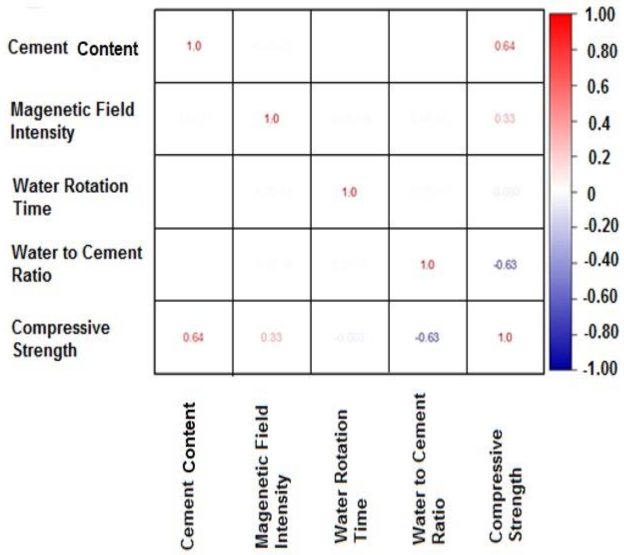

Fig. 4 Correlation matrix for input/output variables.

Figure 5 shows a histogram plot of the output parameter compressive strength, in which this plot exposes the limited area and the compressive strength as distributed.

3.4.2 Training ANN-LM hybrid model

In feed-forward neural networks, otherwise known as multilayer perceptrons, the input vector of independent variables pi is related to the target ti (reflective thinking score). Fig. 6 shows the planning of ANN-LM as used in this study. This figure shows one normally used network, the layered feed-forward neural network with one hidden layer. In this study, a single-hidden-layer feed-forward neural network was utilized, as it proved sufficient for achieving satisfactory performance, taking into account the complexity of the data and the desired level of accuracy in the specific problem context. Every single neuron is linked to those of an earlier layer through adaptable synaptic weights.[27] Knowledge is typically kept as a set of assembly weights. Training is the procedure of adopting the network through a learning mode where input parameters are presented to the network with the desired output, and subsequently, the network weights are regulated so that the network aims to create the anticipated output. The weights after training comprise significant information, whereas before training, they have no meaning and are random.

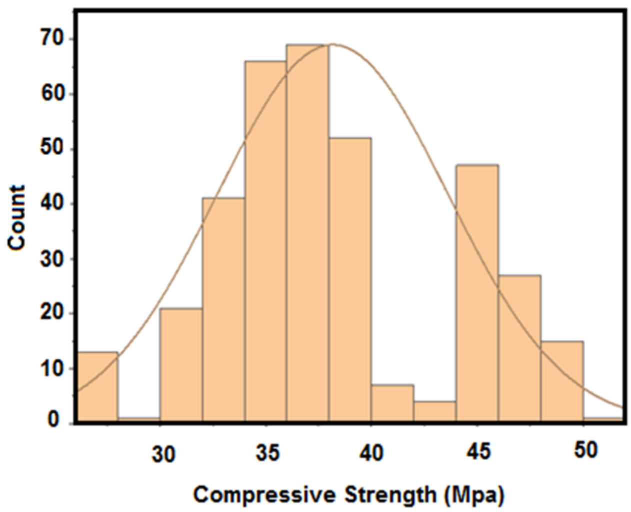

Fig. 5 Distributed concrete compressive strength.

3.4.3 Performance Measures

The Levenberg–Marquardt training procedure was used in all networks. Besides, various statistical metrics containing the mean absolute relative error (MARE), mean squared error (MSE), variance accounted for (VAF), and coefficient of determination (R^2), were applied to examine the performance of the ANN-LM model.[28]

$$MARE = \frac{1}{n}\sum_{i=1}^{n}\left|\frac{P_i - A_i}{A_i}\right| \tag{6}$$

$$MSE = \frac{1}{n}\sum_{i=1}^{n}(P_i - A_i)^2 \tag{7}$$

$$VAF = 1 - \frac{var(P-A)}{var(A)} \tag{8}$$

$$R^2 = \frac{(cov(P,A))^2}{var(P)\cdot var(A)} \tag{9}$$

where n is the sample number; A_i denotes the actual value; $\bar{A}$ represents the mean (average) of actual value; P_i denotes its prediction.

Finally, the function *var()* represents the variance of an individual parameter, while the function *covar()* symbolizes the covariance of two parameters. It is noted that in the case of an ideal match between actual and predicted values, it is recalled that the above metrics take the values of $MARE$= 0, MSE= 0, VAF= 1 (or 100%), and R^2= 1, respectively.

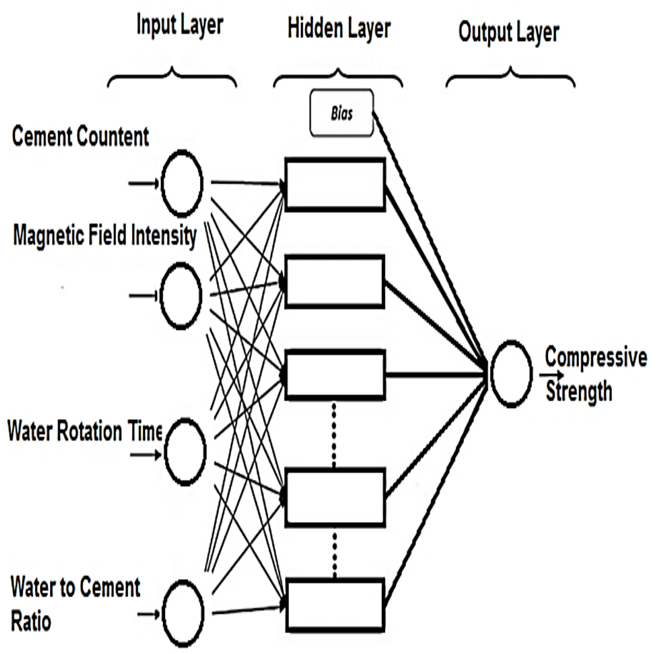

Fig. 6 Structure of Levenberg–Marquardt model.

4. Results and discussion

4.1 Experimental results

Figure 7 presents the measured concrete compressive strength variations in accordance with test parameters. As the MFI increases from 0 to 1.2 Tesla, the compressive strength increases by about 10%. On the other hand, a rather weak effect of circulation time on the compressive strength was observed, as it can be noted at selected intervals of 15, 25, 35, and 65 minutes, respectively. As it was expected, finally, a significant increase in compressive strength was found by increasing the cement content.

4.2 ANN-LM computational intelligence results

Figure 8 presents a comparison between the experimental results and the corresponding predictions generated by the ANN-LM computational intelligence model employed in this study. The high degree of accuracy achieved by the ANN-LM model is evident, as it provides reliable estimations of the compressive strength. This is further supported by the coefficient of determination, which approaches a value close to 1, indicating a strong correlation between the predicted and experimental values. The successful application of the ANN-LM model demonstrates its potential for predicting compressive strength with high precision and reliability.

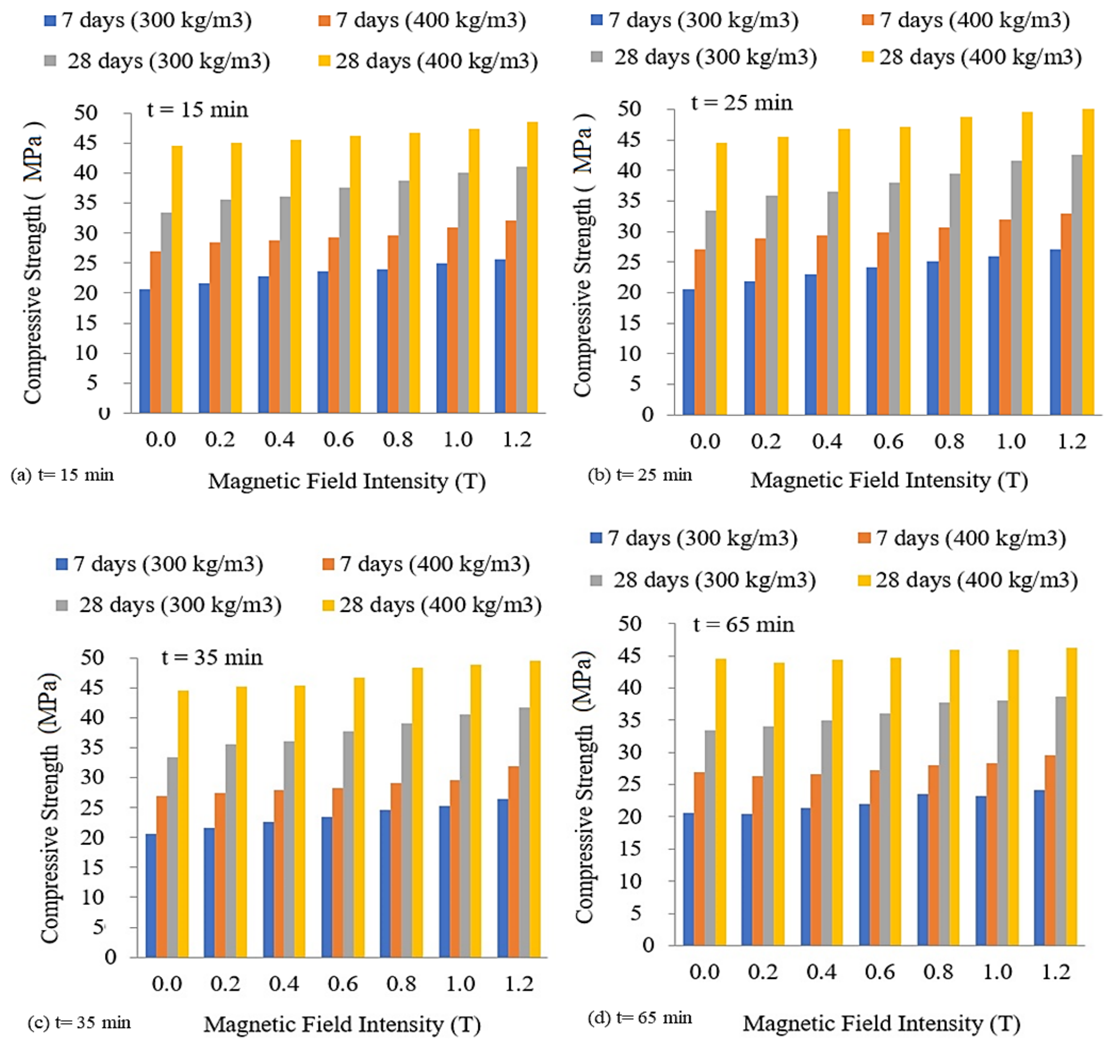

Fig. 7 Effects of cement content, magnetic field intensity, and water circulation time on the compressive strength.

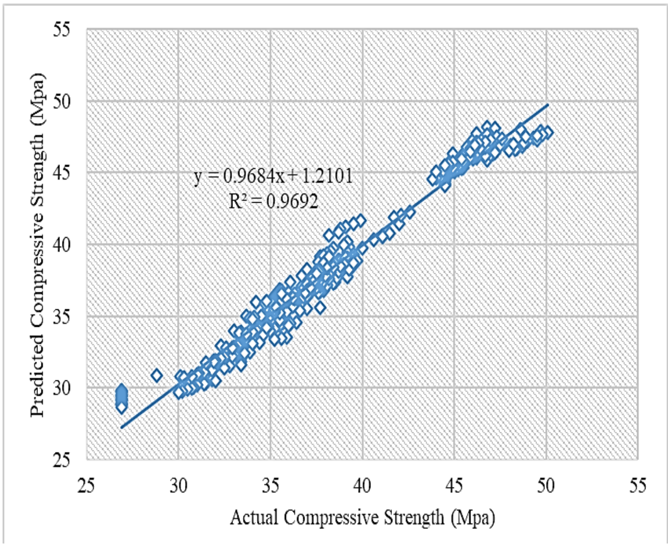

Fig. 8 Comparison of the compressive strength between the experimental results and predictions of Levenberg–Marquardt model.

A GUI has been developed based on the ANN model, as illustrated in Fig. 9. The GUI offers an intuitive and user-friendly platform for users to interact with the model, input relevant parameters, and obtain the predicted results. The interface streamlines the process of applying the ANN model to practical scenarios, enabling users with varying levels of expertise to access the tool and derive meaningful insights.

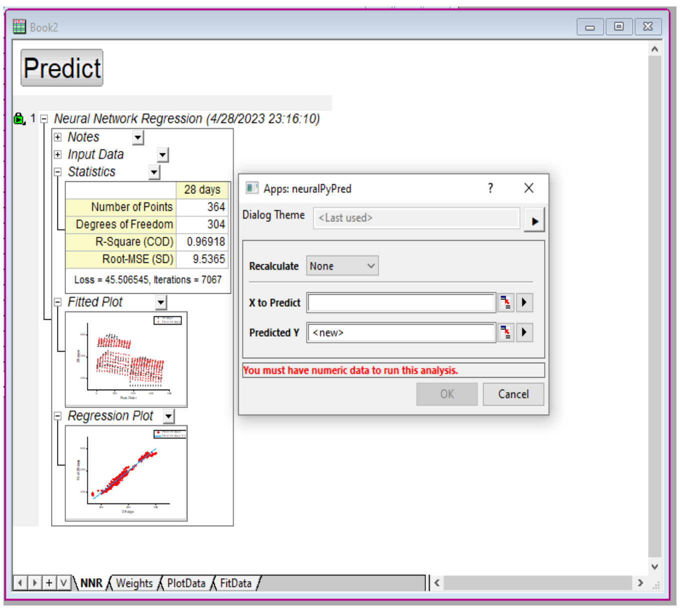

Fig. 9 GUI for the ANN Model - Platform for input parameters and obtain the compressive strength predictions.

To examine the reliability of the hybrid ANN-LM model, a multiple linear regression (MLR) model was also considered (Fig. 10). As explained in section 2.1, in the MLR model, some independent parameters mainly influence the dependent variable. Eq. (10) demonstrates the most appropriate coefficients for the MLR model to evaluate the compressive strength:

$$\begin{aligned}\textit{Compressive strength} &= 45.69313 + 0.069901(\textit{cement content}) + 4.500687(\textit{magnetic field intensity}) \\ &- 0.01734(\textit{water rotation time}) - 68.1758(\textit{water to cement ratio})\end{aligned} \tag{10}$$

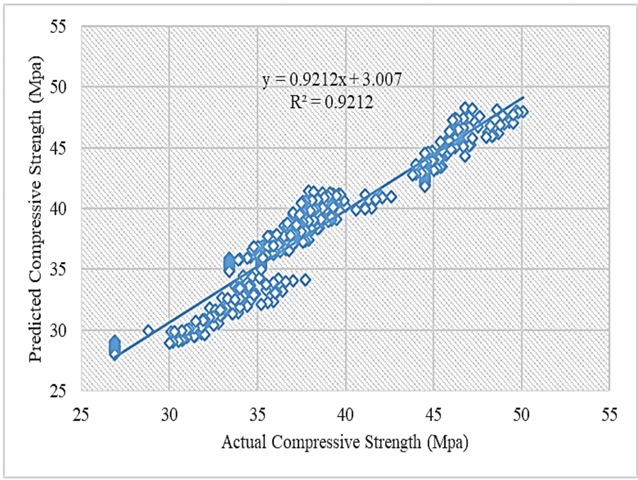

Fig. 10 Comparison of compressive strength between the experimental results and predictions of MLR model.

4.3 Sensitivity analysis of compressive strength

Sensitivity analysis identifies how various values of independent parameters affect a particular dependent parameter under certain assumptions. In other words, sensitivity analyses examine how several origins of uncertainty in an analytical model contribute to the model's global uncertainty. This technique is used within exact boundaries that depend on one or more input parameters.

Sensitivity analysis is used in various fields, ranging from biology and geography to economics and engineering. It is especially useful in studying and analyzing a "Black Box Process" where the output is an opaque function of several inputs. An opaque function or process is one that can't be studied and analyzed for some reason. In general, two types (*i.e.*, local and global) of sensitivity analysis (SA) exist. The former focuses upon the local impact of specific input variables on global performance. The global sensitivity analysis (GSA) examines the effect of a particular input variable over the entire 3-D range and reveals the uncertainty of the output produced by input uncertainty concerning the other variables taken individually.[29] Thus, concerning the nature of the output variables in this study, GSA is more rationale for examining the effect of input variables on the overall model efficiency.

Amongst GSA methods, a variance-based method has been commonly used by researchers for SA. The technique provides an exact methodology for defining each ANN model input parameter's total and first-order sensitivity indices. Assuming a model with form $Y = f(X_1, X_2, \ldots, X_k)$, in which Y is a scalar, to evaluate the impact of individual parameters, the variance-based method takes a variance ratio through variance decomposition based on:[29]

$$V = \sum_{i=1}^{k} V_i + \sum_{i=1}^{k}\sum_{j>i}^{k} V_{ij} + \cdots + V_{1,2,\ldots,k} \quad (11)$$

where V is the variance of the output of the ANN model; V_i is the first-order variance of the input X_i; and V_{ij} to $V_{1,2,\ \ldots,\ k}$ indicates the variance of the interface of the k parameters. V_i and V_{ij} denote the significance of the individual input to the output variance, which is defined as a function of the provisional expectation variance:

$$V_i = V_{x_i}\left[E_{x_{\sim i}}(YX_i)\right] \quad (12)$$

$$V_{ij} = V_{x_i x_j}\left[E_{x_{\sim ij}}(YX_i, X_j)\right] - V_i - V_j \quad (13)$$

and $X_{\sim i}$ determines the set of all input variables in addition to X_i. The first-order sensitivity index (S_i) denotes the first-order effect of an input X_i on the global output, where:

$$S_i = \frac{V_i}{V(Y)} \quad (14)$$

Figure 11 shows the V_{ij} sensitivity analysis result using a tornado diagram. A tornado diagram is a common tool used to depict the sensitivity of a result to changes in selected variables, which shows the effect on the output of varying each input variable at a time, keeping all the other input variables at their initial (nominal) values. Tornado charts map plotted over two bar charts; each bar characterizes the value of the independent parameter. However, each chart is shaded consistent with the "uncertainty", enabling to determination of the uncertainty's impact on the independent parameter's value.

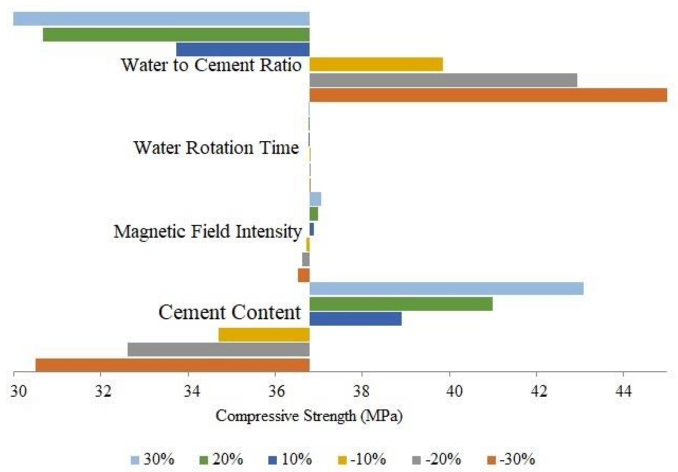

Fig. 11 Tornado diagram of compressive strength to mix design and magnetic water treatment.

Each bar in the two charts is drawn opposite its corresponding bar, extending from the center value outward. The center on the *x*-axis is the minimum value in the data set; this may be a negative or positive value dependent on the data set.

The comparative results confirm that the cement content and water-cement ratio significantly influence the expected compressive strength. For instance, 30% increase in cement content resulted in an increase of compressive strength by around 18%, while decreasing the cement content by 30% decreased the compressive strength by around 19%. The effect of the water-to-cement ratio is more evident where the decrease of this parameter by 30% increased the compressive strength by around 25%. Furthermore, the results indicate that the compressive strength is less sensitive to the magnetic field intensity, in which the increase of this parameter by 30% increases the compressive strength by only around 2.5%. The water circulation time has almost no obvious effect on the compressive strength.

5. Conclusions and future works

This study aimed to investigate the effect of magnetically treated Caspian Seawater on the compressive strength of concrete, and to develop a hybrid artificial neural network coupled with the Levenberg-Marquardt algorithm (ANN-LM) model for estimating the compressive strength in response to various parameters. The research involved in testing a total of 364 concrete cubes with different water-to-cement ratios, magnetic field intensities, water circulation times, and cement contents. The main findings of present study can be summarized as follows:

i. By using magnetically treated Caspian Seawater, an acceptable compressive strength (of around 45 MPa) can be achieved. However, the current technology is more suitable for non-structural applications (with fiber reinforcement polymer) due to the high $MgSO_4$ and $CaSO_4$ content, leading to sulfate resistance issues.

ii. The developed ANN-LM model, supported by a user-friendly GUI, demonstrated reliable and robust results for compressive strength determination, outperforming the MLR model, based on various statistical metrics. The proposed ANN-LM informational model can provide a more accurate, safe, and reliable estimation of compressive strength for similar mix designs, simplifying the design process and offering a more generalized approach for future generative design procedures driven by artificial intelligence.

iii. The sensitivity analysis revealed that the compressive strength is significantly dependent on cement content and water-to-cement ratio, while it is less sensitive to magnetic water treatment parameters, with magnetic field intensity and water circulation time having a significance of 0.02% and 0.006%, respectively.

As major limitations of present study, the research focused on the estimation of compressive strength for magnetized concrete with cement content of 300 and 400 kg/m^3. Future studies could investigate different cement content levels, to enable a broader comparison of strength results. Additionally, the study used Caspian Seawater, but further research extensions could explore the effects of salty water from other seas or oceans. Other factors such as workability, durability, modulus elasticity, and tensile strength could be also investigated and predicted in future studies. In terms of modeling, researchers or designers can explore alternative hybrid ANN models, such as grey wolf optimization-ANN and whale optimization algorithm-ANN, to assess the power and applicability of different optimization techniques for predicting the compressive strength of magnetized concrete.

Conflict of Interest

There is no conflict of interest.

Supporting Information

Not applicable.

References

[1] M. Mazloom, S. M. Miri, Interaction of magnetic water, silica fume and superplasticizer on fresh and hardened properties of concrete, *Advances in Concrete Construction*, 2017, **5**, 87-99, doi: 10.12989/acc.2017.5.2.087.

[2] H. Ahmed, Behavior of magnetic concrete incorporated with Egyptian nano alumina, *Construction and Building Materials*, 2017, **150**, 404-408, doi: 10.1016/j.conbuildmat.2017.06.022.

[3] I. Abavisani, O. Rezaifar, A. Kheyroddin, Magneto-electric control of scaled-down reinforced concrete beams, *ACI Structural Journal*, 2017, **114**, 233-244, doi: 10.14359/51689452.

[4] N. Su, C.-F. Wu, Effect of magnetic field treated water on mortar and concrete containing fly ash, *Cement and Concrete Composites*, 2003, **25**, 681-688, doi: 10.1016/S0958-9465(02)00098-7.

[5] S. Ghorbani, M. Gholizadeh, J. de Brito, Effect of magnetized water on the mechanical and durability properties of concrete block pavers, *Materials*, 2018, **11**, 1647, doi: 10.3390/ma11091647.

[6] R. Dharmaraj, G. K. Arunvivek, A. Karthick, V. Mohanavel, B. Perumal, S. Rajkumar, Investigation of mechanical and durability properties of concrete mixed with water exposed to a magnetic field, *Advances in Civil Engineering*, 2021, **2021**, 1-14, doi: 10.1155/2021/2821419.

[7] B. E. Jouzdani, M. Reisi, Effect of magnetized water characteristics on fresh and hardened properties of self-compacting concrete, *Construction and Building Materials*, 2020, **242**, 118196, doi: 10.1016/j.conbuildmat.2020.118196.

[8] H. Wei, Y. Wang, J. Luo, Influence of magnetic water on early-age shrinkage cracking of concrete, *Construction and Building Materials*, 2017, **147**, 91-100, doi: 10.1016/j.conbuildmat.2017.04.140.

[9] A. R. Esfahani, M. Reisi, B. Mohr, Magnetized water effect on compressive strength and dosage of superplasticizers and water in self-compacting concrete, *Journal of Materials in Civil Engineering*, 2018, **30**, 04018008, doi: 10.1061/(asce)mt.1943-5533.0002174.

[10] Y. H. O. AL-Juboory, A. H. Mahdi, Treating Groundwater Salinity using Magnetic Field Technology, *Systematic Reviews in Pharmacy*, 2020, **11**, 118-123, doi: 10.31838/srp.2020.9.20.

[11] N. Su, Y.-H. Wu, C.-Y. Mar, Effect of magnetic water on the engineering properties of concrete containing granulated blast-furnace slag, *Cement and Concrete Research*, 2000, **30**, 599-605, doi: 10.1016/S0008-8846(00)00215-5.

[12] A. M. Rashad, M. Ezzat, A Preliminary study on the use of magnetic, Zamzam, and sea water as mixing water for alkali-activated slag pastes, *Construction and Building Materials*, 2019, **207**, 672-678, doi: 10.1016/j.conbuildmat.2019.02.162.

[13] R. Malathy, K. Narayanan, P. Mayakrishnan, Performance of prestressed concrete beams using magnetic water for concrete mixing, *Journal of Adhesion Science and Technology*, 2022, **36**, 666-684, doi: 10.1080/01694243.2021.1936383:

[14] M. Ramalingam, K. Narayanan, A. Masilamani, P. Kathirvel, G. Murali, N. I. Vatin, Influence of magnetic water on concrete properties with different magnetic field exposure times, *Materials*, 2022, **15**, 4291, doi: 10.3390/ma15124291.

[15] D. J. Livingstone, D. T. Manallack, I. V. Tetko, Data modelling with neural networks: advantages and limitations, *Journal of computer-aided molecular design*, 1997, **11**, 135-142, doi: 10.1023/A:1008074223811.

[16] M. R. Khosravani, S. Nasiri, D. Anders, K. Weinberg, Prediction of dynamic properties of ultra-high performance concrete by an artificial intelligence approach, *Advances in Engineering Software*, 2019, **127**, 51-58, doi: 10.1016/j.advengsoft.2018.10.002.

[17] Dingqiang, Fan, Precise design and characteristics prediction of Ultra-High Performance Concrete (UHPC) based on artificial intelligence techniques, *Cement and Concrete Composites*, 2021, **122**, 104171, doi: 10.1016/j.cemconcomp.2021.104171.

[18] D. Dao, H.-B. Ly, S. Trinh, T.-T. Le, B. Pham, Artificial intelligence approaches for prediction of compressive strength of geopolymer concrete, *Materials*, 2019, **12**, 983, doi: 10.3390/ma12060983.

[19] Y. Feng, M. Mohammadi, L. Wang, M. Rashidi, P. Mehrabi, Application of artificial intelligence to evaluate the fresh properties of self-consolidating concrete, *Materials*, 2021, **14**, 4885, doi: 10.3390/ma14174885.

[20] M. Wu, L. Zhong, B. Xu, N. Xiong, A consensus-based diffusion levenberg-marquardt method for collaborative localization with extension to distributed optimization, *IEEE Access*, 2020, **8**, 215649-215660, doi: 10.1109/ACCESS.2020.3041491.

[21] Sanwar, Ahmad, Comparison of statistical inversion with iteratively regularized Gauss Newton method for image reconstruction in electrical impedance tomography, *Applied Mathematics and Computation*, 2019, **358**, 436-448, doi: 10.1016/j.amc.2019.03.063.

[22] H. P. Gavin, The Levenberg-Marquardt algorithm for nonlinear least squares curve-fitting problems, Department of Civil and Environmental Engineering, Duke University, 2019, 19, https://people.duke.edu/~hpgavin/lm.pdf.

[23] O. Nelles, Nonlinear System Identification: From Classical Approaches to Neural Networks, Fuzzy Models, and Gaussian Processes. Cham: Springer International Publishing, 2020, doi: 10.1007/978-3-030-47439-3.

[24] D. W. Marquardt, An algorithm for least-squares estimation of nonlinear parameters, *Journal of the Society for Industrial and Applied Mathematics*, 1963, **11**, 431-441, doi: 10.1137/0111030.

[25] R. Toushmalani, Comparison result of inversion of gravity data of a fault by particle swarm optimization and Levenberg-Marquardt methods, *SpringerPlus*, 2013, **2**, 462, doi: 10.1186/2193-1801-2-462.

[26] V. S. Tuzhilkin, D. N. Katunin, Y. R. Nalbandov, Natural

chemistry of caspian sea waters, *The Caspian Sea Environment*, 2005, **5P**, 83-108, doi: 10.1007/698_5_005.
[27] M. Kayri, Predictive abilities of Bayesian regularization and levenberg-marquardt algorithms in artificial neural networks: a comparative empirical study on social data, *Mathematical and Computational Applications*, 2016, **21**, 20, doi: 10.3390/mca21020020.
[28] C. J. Willmott, K. Matsuura, Advantages of the mean absolute error (MAE) over the root mean square error (RMSE) in assessing average model performance, *Climate Research*, 2005, **30**, 79-82, doi: 10.3354/cr030079.
[29] A. Saltelli, M. Ratto, T. Andres, F. Campolongo, J. Cariboni, D. Gatelli, M. Saisana, S. Tarantola, Global sensitivity analysis: the primer, John Wiley & Sons, 2008, doi: 10.1002/9780470725184.

